Thermodynamic analysis of the copper production step in a copper–chlorine cycle for hydrogen production

Mehmet F. Orhan, Ibrahim Dincer*, Marc A. Rosen

Faculty of Engineering and Applied Science, University of Ontario Institute of Technology, 2000 Simcoe Street North, Oshawa, Ontario L1H 7K4, Canada

ARTICLE INFO

ABSTRACT

The hybrid copper–chlorine (Cu–Cl) thermo/electrochemical cycle for decomposing water into its constituents is a novel method for hydrogen production. The process involves a series of closed-loop chemical reactions. The cycle is assumed driven in an environmentally benign manner using nuclear energy. The cycle involves five steps of which three are thermally driven chemical reactions and one has an electrochemical reaction. In the present study, the electrochemical reaction, copper (Cu) production step, is described with its operational and environmental conditions, and analyzed thermodynamically. Various parametric studies are carried out on energetic and exergetic aspects of the step, considering variable reaction and reference-environment temperatures. At a reaction temperature of 45 °C, the reaction heat of the Cu production step is 140,450 kJ/kmol H_2. At a constant reaction temperature of 45 °C, the exergy destruction of the step varies between 50 kJ/kmol H_2 and 7000 kJ/kmol H_2 when the reference-environment temperature increases from 0 °C to 30 °C. At a reaction temperature of 45 °C and a reference-environment temperature of 25 °C, the exergy efficiency of this step is 99% and decreases with increasing reference-environment and/or reaction temperatures.

© 2008 Elsevier B.V. All rights reserved.

1. Introduction

Energy is essential for biological existence. Historical trends of energy consumption suggest that population growth rate may be viewed as dependent on two main parameters: culture and standard of living. Accordingly the role of energy sources is changing as the standard of living of the developing world rises. Fossil fuels account for about 80% of the world annual energy demands while renewables contribute 14% and nuclear 6% [1]. As fossil fuels become scarcer, the demand for new and renewable sources of energy is expected to increase and ultimately dominate.

Recently, global warming due to the greenhouse effect, which is widely considered to be a result of emissions of carbon dioxide and other greenhouse gases, has become a serious environmental problem. Consequently, the development of new environmentally benign energy sources and devices is anticipated to accelerate, so as to address the world's energy and environmental situation.

Hydrogen is currently promoted as a possible future energy carrier. It can be converted with high efficiency to electricity in a fuel cell without any emissions to air except water vapour. In addition, hydrogen has advantageous properties as an energy carrier including being convenient to use, transport and store, and being producible from a widely available raw material (water). Environmental harm does not occur when hydrogen is used, provided it is produced from environmentally benign energy sources (e.g., Ref. [2]).

Extensive research on ways to meet potential hydrogen demands is being conducted, mainly focusing on effective ways to produce hydrogen. Sources of energy are needed from which hydrogen can be produced in large quantities, in an environmentally benign manner and at low cost. The primarily renewable sources such as solar, wave, tidal, hydraulic and wind do not yet meet these requirements. In contrast, nuclear energy can be used, because significant fuel reserves exist for nuclear power and electricity, heat, and hydrogen can be produced from nuclear power with little effect on the environment.

Several methods to produce H_2 are under development. Hydrogen can be produced from fossil fuels and biomass. Also, hydrogen can be generated from water via electrolysis, or thermochemical

Nomenclature

$\bar{e}$	specific energy (kJ/kmol)
E	energy (kJ)
Ex	exergy (kJ)
$\overline{ex}^{ch}$	specific chemical exergy (kJ/kmol)
$\bar{g}$	specific Gibbs free energy (kJ/kmol)
$\bar{g}_f^0$	specific Gibbs free energy of formation (kJ/kmol)
G	Gibbs function (kJ)
h	specific enthalpy (kJ/kg)
$\bar{h}$	specific enthalpy (kJ/kmol)
H	total enthalpy (kJ)
$\bar{h}^0$	specific enthalpy at reference state (kJ/kmol)
$\bar{h}_f^0$	specific enthalpy of formation (kJ/kmol)
$\dot{m}$	mass flow rate (kg/s)
n	number of moles per cycle (kmol/kmol H_2)
$\bar{q}$	specific reaction heat (kJ/kmol)
Q	heat (kJ)
s	specific entropy (kJ/(kg K))
$\bar{s}$	specific entropy (kJ/(kmol K))
$\bar{s}^0$	specific entropy at reference state (kJ/(kmol K))
$\bar{s}_f^0$	specific entropy of formation (kJ/(kmol K))
$T_{reaction}$	reaction temperature (K)
T_0	reference-environment temperature (K)
u	specific internal energy (kJ/kg)
V	velocity (m/s)
z	elevation (m)

Greek letters

ΔG	change in Gibbs function for a reaction (kJ)
η_{ex}	exergy efficiency

decomposition. Some of these processes are commercially available, while significant development work is required for others before they can be commercialized. The potentially viable H_2 production methods impose a set of difficult requirements on a nuclear reactor, including delivery of heat at a near-constant high temperature, isolation of the reactor from the H_2 production facility, and low-pressure-coolant interfaces between the reactor and the H_2 production facility. Current reactor technology can be modified to meet these requirements, but the severity of the requirements suggests that the nuclear reactor should be designed to match chemical plant requirements. Significant development will likely be required of both the H_2 production methods and the corresponding nuclear reactor systems to achieve optimal combined systems. Many types of nuclear reactors have the potential capabilities to match H_2 production requirements. One example is nuclear hydrogen production using the high-temperature gas-cooled reactor (HTGR), being developed by the Japan Atomic Energy Research Institute (JAERI), as described by Onuki et al. [3]. The reactor technology has been developed using the high-temperature engineering test reactor (HTTR) installed at JAERI's Oarai location. The HTTR reached its full operating power of 30 MW in 2001 and reported a reactor outlet helium temperature of 950 °C in April 2004. The corresponding hydrogen-production technology under development at JAERI is the thermochemical sulfur–iodine (SI) process.

The HTGR represents an advantageous concept for efficient, economic and safe nuclear power generation in the future. Its potential to produce heat at high temperatures can be utilized in many industrial processes for the generation of hydrogen or other synthetic chemical fuels, which may find broadening application in future global energy markets. Verfondern and Lensa [4] describe

German long-term activities in the "Prototype Nuclear Process Heat Reactor Project", in which the technical feasibility of an HTGR in combination with coal gasification has been demonstrated, and in "Nuclear Long Distance Energy Transportation". High-temperature helium-cooled reactors appear to be the most well understood nuclear technology that can supply high-temperature heat for thermal processes for producing hydrogen. The GT-MGR reactor, an innovative international modular design of a helium-cooled reactor with a gas-turbine cycle, meets the requirements for hydrogen production and has been proposed as a basis for a nuclear energy source [5]. Technical aspects of the proposed HTGR application for producing hydrogen have been analyzed by Mitenkov et al. [5], who determined the required energy parameters for the HTGR for present and future hydrogen-production technologies. Challenges and additional research needs relating to the HTGR at high helium temperatures are identified.

Forsberg [6] indicates that the infrastructure for H_2 use is compatible with the production of H_2 by nuclear reactors. By examining alternative H_2 production processes, he defines the requirements such processes would impose on the nuclear reactor, including supplying heat at a near-constant high temperature, providing a low-pressure interface with the H_2 production processes, isolating the nuclear plant from the chemical plant, and avoiding tritium contamination of the H_2 product. The advanced high-temperature reactor (AHTR) concept was developed to match these requirements for H_2 production.

Nishihara and Inagaki [7] summarize research activities on hydrogen production using the HTTR. A key issue for the HTTR hydrogen-production system is the development of a control technology for stable operation. A thermal load absorber using a steam generator installed downstream of the reformer is proposed to protect against variations in helium temperature. Thermal–hydraulic analyses during start-up and the suspension of the feed gas supply to the reformer are carried out. Their results show that the reformer outlet helium temperature varies notably with a change in the feed gas flow rate. However, the steam generator can mitigate the variation in helium temperature. Hence, the HTTR can continue normal operation independently of the feed gas flow rate.

Research on system integration has been carried out by Inagaki et al. [8] in four areas: control technology to maintain reactor operation despite thermal disturbances caused by the hydrogen-production system, estimation of tritium permeation into the hydrogen from the reactor, a countermeasure against explosion, and development of a high-temperature valve to isolate the reactor and hydrogen-production systems in the event of an accident.

The molten salt-cooled AHTR is a new reactor concept designed to provide high-temperature (750–1000 °C) heat to enable efficient low-cost thermochemical production of hydrogen or production of electricity. Forsberg et al. [9] provide an initial description and technical analysis of its key features. The proposed AHTR uses coated-particle graphite-matrix fuel similar to that used in HTGRs, such as the General Atomic gas turbine–modular helium reactor. However, unlike the HTGRs, the AHTR uses a molten-salt coolant and a pool configuration, similar to that of the General Electric Super Power Reactor Inherently Safe Module liquid-metal reactor. Because the boiling points for molten fluoride salts are near 1400 °C, the reactor can operate at very high temperatures and atmospheric pressure. For thermochemical H_2 production, the heat is delivered at the required near-constant high temperature and low pressure. For electricity production, a multi-reheat helium Brayton (gas turbine) cycle, with efficiencies exceeding 50%, is used. The low-pressure molten-salt coolant, with its high heat capacity and natural circulation heat transfer capability, creates the potential for robust safety (including fully passive decay-heat removal) and
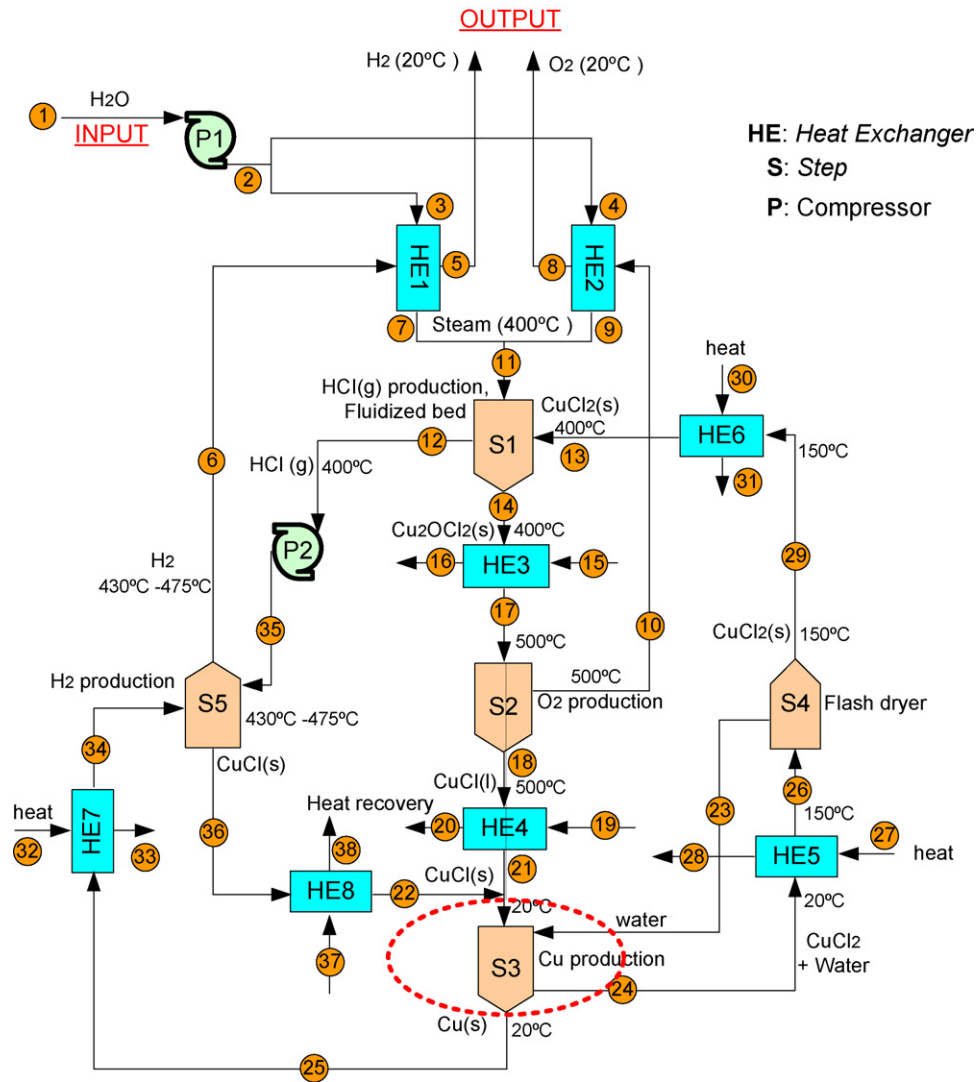
Fig. 1. Conceptual layout of a thermochemical Cu–Cl hydrogen production cycle, showing the Cu production step assessed in this article in a dashed oval.

improved economics with passive safety systems that allow higher power densities and scaling to large reactor sizes (over 1000 MW electric).

This splitting of water can be achieved through direct electrolysis or via one of the several thermochemical cycles where the net reaction is the decomposition of water. Thermochemical cycles aim to avoid the Carnot efficiency limitations in the production of electricity from thermal energy, and thus can potentially have higher efficiency than the electrolytic process. However, this higher potential efficiency may not be realized because of the complexity and poor selectivity of the proposed thermochemical systems. As a result, the electrolytic decomposition of water, a relatively well-known and established technology, may prove superior to thermochemical cycles. Many types of thermochemical processes for H_2 production exist. A demonstration experiment for hydrogen production was carried out for a SI thermochemical water decomposition process on a laboratory scale by Xinxin and Kaoru [10]. The results confirmed the feasibility of the closed-loop operation for recycling all reactants, except for water, H_2 and O_2. Membrane technology was developed to enhance the decomposition efficiency. The maximum attainable one-pass HI conversion rate was reported to exceed 90% with membrane technology, whereas the equilibrium rate is about 20%.

Hydrogen production with a fast breeder reactor may be an attractive option as a long-term energy source with nuclear fuel breeding. The thermochemical and electrolytic hybrid hydrogen-production process using a sulfuric acid cycle requires a maximum temperature of 500 °C, which can be supplied by a sodium-cooled fast breeder reactor [11]. In that study, a hydrogen-production plant using thermochemical and electrolytic hybrid processes is designed by Chikazawa et al. [11], and the hydrogen-production efficiency is evaluated. The structural materials of the components in the system are steels such as high-Si cast iron, which has a good resistance to sulfuric acid. A high efficiency for hydrogen production of 44% (based on higher heating value) can be achieved, assuming the development of high efficiency electrolysis.

Most thermochemical cycles require process heat at high temperatures, exceeding 850–900 °C. Recently, Atomic Energy of Canada Limited and Argonne National Laboratory in the U.S. have been developing a low-temperature cycle, to accommodate heat sources around 500–550 °C. Such cycles can be more readily integrated with nuclear reactors. For this temperature range, the copper–chlorine (Cu–Cl) cycle is one of the most promising. Several Cu–Cl cycles have been examined in the laboratory and various alternative configurations identified. This hydrogen-production cycle consists of a series of chemical reactions in which

water is split into hydrogen and oxygen, through reactions involving intermediate copper and chlorine compounds, which are recycled. Proof-of-principle experiments that demonstrate the feasibility of the process have been undertaken and a preliminary assessment of the cycle efficiency demonstrated [12]. This study, as noted earlier, focuses on the Cu production step of the Cu–Cl cycle.

The objectives of this study are to describe the copper production step of the Cu–Cl cycle for hydrogen production, to perform a thermodynamic analysis of the step accounting for relevant chemical reactions and including the determination of energy and exergy efficiencies, and to perform various parametric studies on energetic and exergetic aspects of the step, considering various reaction and reference-environment temperatures.

2. System description

A conceptual layout of a Cu–Cl process is illustrated in Fig. 1. Thermochemical water decomposition, potentially driven by nuclear heat, splits water into hydrogen and oxygen through the cycling of intermediate copper and chlorine compounds. This cycle consists of three main thermally driven chemical reactions and one electrochemical reaction. The cycle involves five main steps: (1) HCl(g) production using such equipment as a fluidized bed, (2) oxygen production, (3) copper (Cu) production, (4) drying and (5) hydrogen production. A chemical reaction takes place in each step, except drying. The chemical reactions form a closed internal loop that re-cycles all of the Cu–Cl compounds on a continuous basis, without emitting any greenhouse gases to the atmosphere. The five steps the Cu–Cl cycle are described in Table 1.

As illustrated in Fig. 1, only water and nuclear-derived heat/electricity enter the cycle and at the end of the process only H_2 and O_2 are produced (with no greenhouse gas emissions). Liquid water at ambient temperature enters the cycle and passes through several heat exchangers where it evaporates and increases in temperature to 400 °C. Heat for this process is obtained from cooling the hydrogen and oxygen gases before they exit the cycle. Steam at 400 °C and solid copper chloride ($CuCl_2$) at 400 °C from the dryer enter the fluidized bed, where a chemical reaction occurs. This reaction is endothermic and yields hydrochloric gas (HCl) and Cu_2OCl_2. Hydrochloric gas is compressed and Cu_2OCl_2 is transferred to another process step after its temperature is increased to the oxygen production reaction temperature of 500 °C.

In the second (oxygen production) step an endothermic chemical reaction takes place in which Cu_2OCl_2 is heated and O_2 and copper monochloride (CuCl) are produced. Liquid copper monochloride is solidified by cooling it to 20 °C, after which it enters the third (copper production) step together with the solid copper monochloride from the fifth step. In the third process step, as illustrated in Fig. 2, solid copper monochloride and water react endothermically at 20 °C. However in this reaction water acts as a catalyst, and does not react with the other elements or compounds. The chemical formula for this reaction is given by:

$$4CuCl(s) + H_2O(l) \xrightarrow{Q} 2CuCl_2(s) + 2Cu(s) + H_2O(l)$$

Another specification for this third reaction that differentiates this step from others and makes it the most expensive, based on the price of electricity, is that electrolysis occurs. In this reaction, solid copper and a copper chloride–water solution are produced. A mixture of copper chloride and water is transferred to the dryer, and solid copper enters the fifth step after its temperature is increased to that step's operating temperature.

In the fifth (hydrogen production) step, hydrochloric gas and copper enter, and are converted to hydrogen gas (H_2) and solid copper monochloride (CuCl). The reaction takes place at 450 °C at steady state.

3. Analysis

During the analysis, we consider 1 kmol of hydrogen produced per cycle, so all quantities are provided per kmol of hydrogen produced. Also, we assume that the reference-environment temperature (T_0) and pressure (P_0) are 25 °C and 1 atm, respectively. The reactants and products for the chemical reaction are at the reaction temperature and a pressure of 1 atm. The process occurs at steady state, is adiabatic and proceeds to completion.

Mass is conserved in chemical reactions, as the masses of products and reactants are equal, so a general steady-state mass rate balance can be expressed as follows:

$$\dot{m}_{in} = \dot{m}_{out} \quad or \quad \dot{m}_{reactants} = \dot{m}_{products} \tag{1}$$

Based on Fig. 2, a mass balance for the Cu production step can be written as follows:

$$n_{21}\bar{m}_{21} + n_{22}\bar{m}_{22} + n_{23}\bar{m}_{23} = n_{24}\bar{m}_{24} + n_{25}\bar{m}_{25} \tag{2}$$

where $\bar{m}$ and n are the molar mass and the mole number of the compound per cycle, respectively.

Several considerations enter when writing energy balances for systems involving chemical reaction. Some of these apply generally, without regard for whether reaction takes place. For example, it is necessary to determine work and heat transfers, as well as the importance of kinetic and potential energy. Other considerations relate to the occurrence of combustion or other reactions. For example, it is important to know the states and conditions of the reactants before reaction occurs, and if they are premixed. The state of the products also must be assessed, e.g., if water formed on reaction has condensed.

Table 1
Key steps of Cu–Cl cycle with their corresponding reactions, highlighting the copper production step studied in the paper.

Step	Reaction	Temperature Range (°C)	Pressure (kPa)	Feed/Output (note: Q-thermal energy, V-electrical energy)	
1	$2CuCl_2(s)+H_2O(g)\rightarrow$ $CuO*CuCl_2(s)+2HCl(g)$	400	101	Feed:	$CuCl_2(s)+H_2O+Q$
				Output:	$CuO*CuCl_2(s)+HCl(g)$
2	$CuO*CuCl_2(s)\rightarrow$ $2CuCl(l)+1/2O_2(g)$	500	101	Feed:	$CuO*CuCl_2(s)+Q$
				Output:	Molten CuCl salt + O_2
3	$4CuCl(s)+H_2O\rightarrow$ $2CuCl_2(aq)+2Cu(s)$	25-80	101	Feed:	CuCl and H_2O + V
				Output:	Cu and slurry
4	$CuCl_2(aq)\rightarrow CuCl_2(s)$	>100	101	Feed:	$CuCl_2(aq)+Q$
				Output:	$CuCl_2+H_2O$ vapors
5	$2Cu(s)+2HCl(g)\rightarrow$ $2CuCl(l)+H_2(g)$	430-475	101	Feed:	Cu + HCl
				Output:	$H_2 + CuCl(l)$ salt+Q

Source: Adapted from Ref. [13].
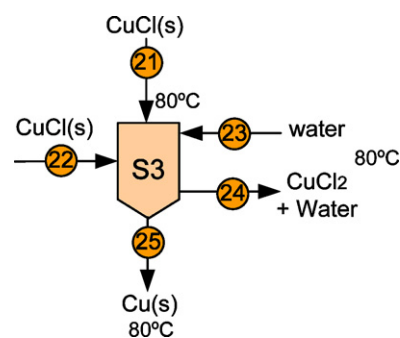
Fig. 2. Cu production step.

The heat transfer for a chemical process involving no work interaction W is determined from the energy balance $\dot{E}_{in} - \dot{E}_{out} = \Delta\dot{E}_{system}$ applied to the system with $W = 0$. For a steady-state reaction process, the energy balance reduces to:

$$Q = H_P - H_R = \sum n_P(\bar{h}_f^0 + \bar{h} - \bar{h}^0)_P - \sum n_R(\bar{h}_f^0 + \bar{h} - \bar{h}^0)_R \qquad (3)$$

The heat transfer for this chemical process can be found with an energy balance:

$$Q = [n(\bar{h}_f^0 + \bar{h} - \bar{h}^0)]_{24} + [n(\bar{h}_f^0 + \bar{h} - \bar{h}^0)]_{25} - [n(\bar{h}_f^0 + \bar{h} - \bar{h}^0)]_{21}$$
$$- [n(\bar{h}_f^0 + \bar{h} - \bar{h}^0)]_{22} - [n(\bar{h}_f^0 + \bar{h} - \bar{h}^0)]_{23} \qquad (4)$$

Exergy analysis, a useful technique for assessing and improving efficiency, is used throughout this analysis [14]. An exergy balance for a process involving chemical reactions can be written as follows:

$$\sum Ex_{in} - \sum Ex_{out} - Ex_{destruction} = \Delta Ex_{system} \qquad (5)$$

For a steady-state process, $\Delta Ex_{system} = 0$. The exergy associated with a flow at a specified state is the sum of thermomechanical and chemical contributions [14]. Thus, the specific exergy of a flow can be expressed as follows:

$$\overline{ex} = \underline{(\bar{h} - \bar{h}_0) - T_0(\bar{s} - \bar{s}_0) + \frac{V^2}{2} + gz} + \overline{ex}^{ch} \qquad (6)$$

Here, the underlined term is the thermomechanical contribution and $\overline{ex}^{ch}$ is the chemical contribution. Combining Eqs. (5) and (6) for a process involving no work interactions yields:

$$\overline{ex}_{destruction} = \sum n\left[(\bar{h} - \bar{h}_0) - T_0(\bar{s} - \bar{s}_0) + \frac{V^2}{2} + gz + \overline{ex}^{ch}\right]_{in}$$
$$- \sum n\left[(\bar{h} - \bar{h}_0) - T_0(\bar{s} - \bar{s}_0) + \frac{V^2}{2} + gz + \overline{ex}^{ch}\right]_{out}$$
$$+ \left(1 - \frac{T_0}{T_{reaction}}\right)Q \qquad (7)$$

where Q, as given in Eq. (4), is the heat flow into the system (negative for exothermic reactions). For the chemical reactions in the Cu–Cl cycle, it is reasonable to assume the specific kinetic exergy ($V^2/2$) and specific potential exergy (gz) of the flows are equal to zero. Then,

$$\overline{ex}_{destruction} = \sum n[(\bar{h} - \bar{h}_0) - T_0(\bar{s} - \bar{s}_0) + \overline{ex}^{ch}]_{in}$$
$$- \sum n[(\bar{h} - \bar{h}_0) - T_0(\bar{s} - \bar{s}_0) + \overline{ex}^{ch}]_{out}$$
$$+ \left(1 - \frac{T_0}{T_{reaction}}\right)Q \qquad (8)$$

Consequently, the corresponding exergy balance for the Cu production step can be written as follows:

$$\overline{ex}_{destruction} = n_{21}[(\bar{h} - \bar{h}_0) - T_0(\bar{s} - \bar{s}_0) + \overline{ex}^{ch}]_{21} + n_{22}[(\bar{h} - \bar{h}_0)$$
$$- T_0(\bar{s} - \bar{s}_0) + \overline{ex}^{ch}]_{22} + n_{23}[(\bar{h} - \bar{h}_0) - T_0(\bar{s} - \bar{s}_0)$$

$$+ \overline{ex}^{ch}]_{23} - n_{24}[(\bar{h} - \bar{h}_0) - T_0(\bar{s} - \bar{s}_0) + \overline{ex}^{ch}]_{24}$$
$$- n_{25}[(\bar{h} - \bar{h}_0) - T_0(\bar{s} - \bar{s}_0)$$
$$+ \overline{ex}^{ch}]_{25} + \left(1 - \frac{T_0}{T_{reaction}}\right)Q \qquad (9)$$

For reacting and nonreacting systems, different methods are used to evaluate thermodynamic properties such as specific internal energy u, enthalpy h and entropy s. In thermodynamic tables for nonreacting system, values for u, h, and s are relative to some arbitrary datum state where these properties are set to zero. This approach is satisfactory for evaluations involving differences in property values between states of the same composition, because then the arbitrary datum cancels. However, when a chemical reaction occurs, reactants change and products are formed, so differences cannot be calculated for all substances involved. For reacting systems, it is necessary to evaluate quantities like h, u, and s so there are no inconsistencies in properties. In this study the enthalpy and entropy values of each compound are evaluated with Shomate equations [15] as follows:

$$\bar{h} - \bar{h}_0 = AT + \frac{BT^2}{2} + \frac{CT^3}{3} + \frac{DT^4}{4} - \frac{E}{T} + F - H \qquad (10)$$

and

$$\bar{s} = A\ln(T) + BT + \frac{CT^2}{2} + \frac{DT^3}{3} - \frac{E}{2T^2} + G \qquad (11)$$

where T is $1/1000$ of the specified temperature (in K) of a compound and A, B, C, D, E, F, G and H are constants, given in Table 2 for compounds relevant to the process being examined.

With the specific enthalpy and entropy values, we can calculate the specific chemical exergy $\overline{ex}^{ch}$ value of each compound. Evaluating the thermomechanical contributions can be viewed as bringing the system without change in composition from the specified state to T_0 and P_0, the condition where the system is in thermal and mechanical equilibrium with the reference-environment. Depending on the nature of the system, this may be a real or hypothetical condition.

The chemical exergy based on a typical reference-environment exhibiting standard values of the reference-environment temperature T_0 and pressure P_0 such as 298.15 K and 1 atm is called standard chemical exergy. To determine the standard chemical exergy of any substance not present in the environment, we consider the reaction of the substance with other substances for which the standard chemical exergies are known, and write:

$$\overline{ex}^{ch} = -\Delta G + \sum_P n\overline{ex}^{ch} - \sum_R n\overline{ex}^{ch} \qquad (12)$$

where ΔG is the change in Gibbs function for the reaction, regarding each substance as separate at temperature T_0 and pressure P_0. The other two terms on the right side of Eq. (12) are evaluated using the known standard chemical exergies, together with values of n, which express the moles of these reactants and products per mole of the substance whose chemical exergy is being evaluated.

For example, the chemical exergy of copper chloride ($CuCl_2$) is obtained from its constituent elements, for which standard chemical exergies are known. The formation reaction for copper chloride

Table 2
Enthalpy of formation, reference entropy and Shomate constants for chemical compounds.

Compound	$\bar{h}_f^0$ (kJ/kmol)	$\bar{s}^0$ (kJ/kmol K)	A	B	C	D	E	F	G	H
$CuCl_2(s)$	−205,850	108.06	70.21882	23.36132	−14.86876	4.053899	−0.366203	−228.9405	184.6378	−205.8532
$CuCl(s)$	−138,070	87.04	75.27100	−26.8321	25.69156	−7.357982	−1.847747	−165.7299	174.6644	−138.0720
$H_2O(l)$	−285,830	69.95	−203.606	1523.290	−3196.413	2474.455	3.855326	−256.5478	−488.716	−285.8304
$Cu(s)$	0	33.17	17.72891	28.09870	−31.25289	13.97243	0.068611	−6.056591	47.89592	0

Table 3
Formation reactions for several compounds in the Cu production step of the Cu–Cl cycle.

Compound	Reaction of formation
H_2O	$H_2 + (1/2)O_2 \rightarrow H_2O$
$CuCl_2$	$Cu + Cl_2 \rightarrow CuCl_2$
$CuCl$	$Cu + (1/2)Cl_2 \rightarrow CuCl$

is given by:
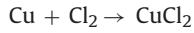
$$Cu + Cl_2 \rightarrow CuCl_2$$

Applying Eq. (12) on a specific basis to this reaction we obtain:

$$\overline{ex}_{CuCl_2}^{ch} = [\bar{g}_{CuCl_2} - \bar{g}_{Cu} - \bar{g}_{Cl_2}]_{(T_0,P_0)} + \overline{ex}_{Cu}^{ch} + \overline{ex}_{Cl_2}^{ch} \tag{13}$$

The change in the specific Gibbs function for this reaction is given by:

$$\bar{g}_P - \bar{g}_R = (\bar{h} - T\bar{s})_{CuCl_2} - (\bar{h} - T\bar{s})_{Cu} - (\bar{h} - T\bar{s})_{Cl_2}$$
$$= (\bar{h}_{CuCl_2} - \bar{h}_{Cu} - \bar{h}_{Cl_2}) - T(\bar{s}_{CuCl_2} - \bar{s}_{Cu} - \bar{s}_{Cl_2}) \tag{14}$$

where $\bar{g}_P$ and $\bar{g}_R$ denote, respectively, the Gibbs function of the reactants and products, per kmol of copper chloride.

For reacting systems, an enthalpy datum can be established by assigning arbitrarily a value of zero to the enthalpy of the stable elements at a state called the standard reference state and defined by $T_0 = 298.15$ K and $P_0 = 1$ atm. Note that only stable elements are assigned a value of zero enthalpy at the standard state. The term stable simply means that the particular element is in a chemically stable form. Using such a datum, enthalpy values can be assigned to compounds for use in the study of reacting systems. The enthalpy of a compound at the standard state equals its enthalpy of formation $\bar{h}_f^0$. The enthalpy of formation is the energy released or absorbed when the compound is formed from its elements, the compound and elements all being at T_0 and P_0. The specific enthalpy of a compound at a state other than the standard state is found by adding the specific enthalpy change between the standard state and the state of interest to the enthalpy of formation.

At the standard reference state, the enthalpies and Gibbs functions for copper (Cu) and chlorine (Cl_2) are zero because they are stable elements at this state. Thus, in Eq. (14):

$$\bar{g}_R = \bar{h}_{Cu} = \bar{h}_{Cl_2} = 0 \quad \text{and} \quad \bar{g}_P = (\bar{g}_f^0)_{CuCl_2}$$

and

$$\bar{g}_P = (\bar{g}_f^0)_{CuCl_2} = (\bar{h}_f^0)_{CuCl_2} - T_0(\bar{s}_{CuCl_2}^0 - \bar{s}_{Cu}^0 - \bar{s}_{Cl_2}^0) \tag{15}$$

where the superscript 0 denotes properties at T_0 and P_0. Combining Eqs. (13) and (15) yields:

$$\overline{ex}_{CuCl_2}^{ch} = (\bar{h}_f^0)_{CuCl_2} - T_0(\bar{s}_{CuCl_2}^0 - \bar{s}_{Cu}^0 - \bar{s}_{Cl_2}^0) + \overline{ex}_{Cu}^{ch} + \overline{ex}_{Cl_2}^{ch} \tag{16}$$

With this procedure, we obtain the standard chemical exergy of other compounds that participate in the Cu production step of the Cu–Cl cycle. The formation reactions for these compounds are given in Table 3, and the specific enthalpy, entropy and Gibbs function of formation of the elements comprising these compounds are given

Table 4
Enthalpy, entropy and Gibbs free energy of formation, and standard chemical exergy of elements.

Elements	$\bar{h}_f^0$ (kJ/kmol)	$\bar{s}^0$ (kJ/kmol K)	$\bar{g}_f^0$ (kJ/kmol)	$\overline{ex}^{ch}$ (kJ/kmol)
O_2	0	205.03	0	3,970
Cu	0	33.17	0	132,600
Cl_2	0	223.08	0	123,600
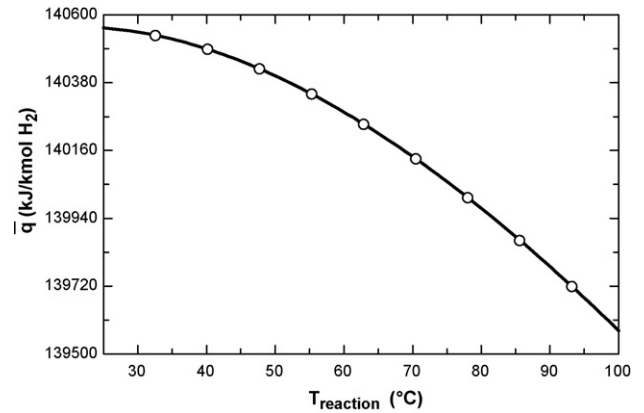
Fig. 3. Variation of reaction heat with reaction temperature for Cu production step in the Cu–Cl cycle.

in Table 4 along with their standard chemical exergies. Standard chemical exergies of all compounds involved in the Cu production step, obtained using these data, are given in Table 5.

An exergy efficiency can be formulated for the reacting system. At steady state, the rate at which exergy enters the reacting system equals the rate at which exergy exits plus the rate at which exergy is destroyed within the system. We assume the reactor is well insulated, so there is no heat transfer and thus no accompanying exergy transfer. There is also no work $\dot{W}_{cv}$, so exergy exits only with the reaction products. An exergy efficiency can be written as follows:

$$\eta_{ex} = \frac{\overline{ex}_{out}}{\overline{ex}_{in}} \tag{17}$$

or, using the exergy balance for the reacting system, as follows:

$$\eta_{ex} = 1 - \frac{\overline{ex}_{destroyed}}{\overline{ex}_{in}} \tag{18}$$

where $\overline{ex}_{in}$ is the specific exergy that enters with the reactants and with heat (which is non-zero in the case of an endothermic reaction), and $\overline{ex}_{out}$ is the specific exergy exiting the system with the products and with heat (which is non-zero in the case of an exothermic reaction).

4. Results and discussion

The first results presented are property data, which are needed in the subsequent analysis. The Gibbs free energy and the standard chemical exergy of selected compounds, which are calculated with Eqs. (15) and (16), respectively, are given in Table 5. These values are based on a reference-environment temperature and pressure of 25 °C and 1 atm, respectively. As illustrated in Table 5, the Gibbs free energy of elements that are stable at this temperature and pressure is zero.

The variation of the reaction heat for the Cu production step, with reaction temperature, is illustrated in Fig. 3. As explained earlier, an endothermic reaction takes place in this step. As reaction

Table 5
Gibbs free energy of formation and standard chemical exergy for compounds involved in the Cu production step of the Cu–Cl cycle.

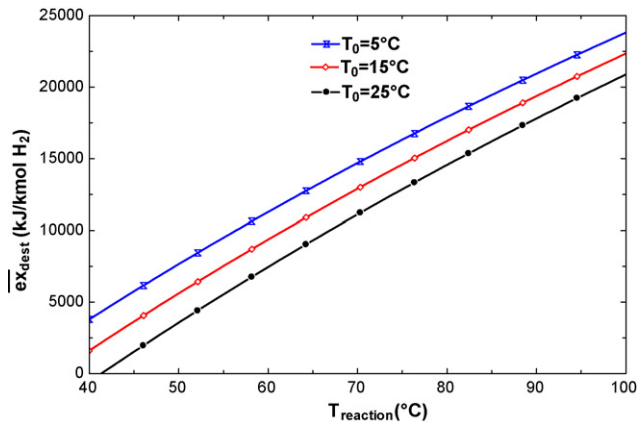| Compound	Specific Gibbs free energy of formation, $\bar{g}_f^0$ (kJ/kmol)	Specific standard chemical exergy, $\overline{ex}^{ch}$ (kJ/kmol)
$CuCl_2(s)$	−161,667	94,533
$CuCl(s)$	−120,876	73,524
$H_2O(l)$	−237,180	900
$Cu(s)$	0	132,600

Fig. 4. Variation of the specific exergy destruction for the Cu production step in the Cu–Cl cycle with reaction temperature, for several reference-environment temperatures.

temperature increases, the reaction heat for the Cu production step decreases nonlinearly.

The variations of specific exergy destruction for the Cu production step with reaction and reference-environment temperatures are shown in Figs. 4 and 5. In these figures, the specific exergy destruction is seen to decrease sharply as reaction temperature decreases and to increase as reference-environment temperature decreases. The relations are approximately linear. Reference-environment temperatures of 5 °C, 15 °C and 25 °C and reaction temperatures of 45 °C, 80 °C and 100 °C are considered.

Inlet and outlet exergies for the Cu production step are illustrated as a function of reaction and reference-environment temperatures in Figs. 6 and 7, respectively. In Fig. 7, the inlet exergy decreases sharply with increasing reference-environment temperature while outlet temperature decreases modestly. The results in Fig. 7 are obtained at a constant reaction temperature of 80 °C. In contrast to Fig. 7, the inlet exergy of reaction is seen in Fig. 6 to increase dramatically with reaction temperature whereas the outlet exergy increases moderately. Because of these effects of reference-environment and reaction temperatures on the inlet and outlet exergies, as illustrated in Figs. 8 and 9, the exergy destruction of the reaction decreases with reference-environment temperature and increases with reaction temperature.

The exergy efficiency of the Cu production step increases approximately linearly as reference-environment temperature
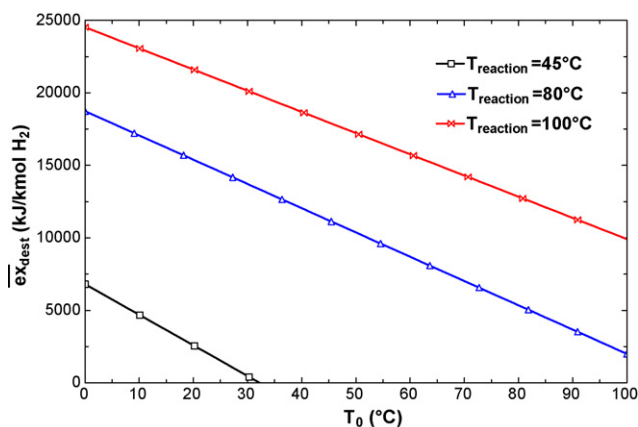

Fig. 6. Change in exergies of the Cu production step before and after reaction with respect to reaction temperature.

Fig. 7. Inlet and outlet exergies of the Cu production step based on reference-environment temperature at reaction temperature of 80 °C.

increases and decreases nearly linearly as reaction temperature increases. These relations are shown in Fig. 10. The exergy efficiency of this step varies between 93% and 99%. The relation of exergy efficiency with reference-environment temperature is obtained for a constant reaction temperature of 80 °C and with reaction temperature is evaluated at a constant reference-environment temperature of 25 °C. The exergy efficiency of the step changes based on the reaction and reference-environment temperatures,

Fig. 5. Variation of the specific exergy destruction for the Cu production step in the Cu–Cl cycle with reference-environment temperature, for several reaction temperatures.
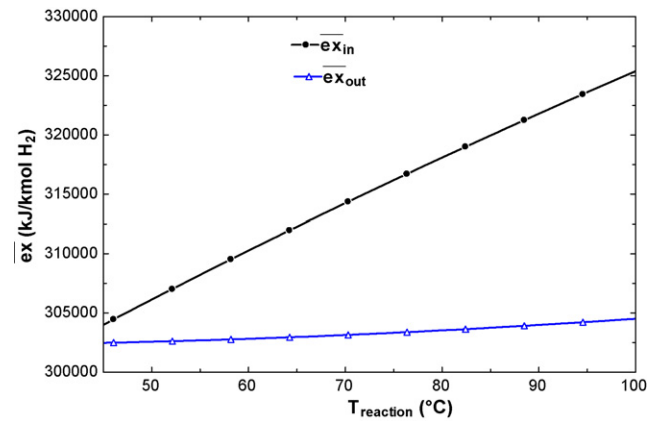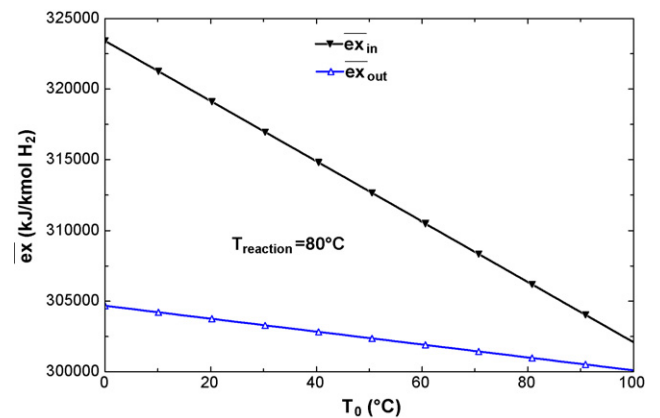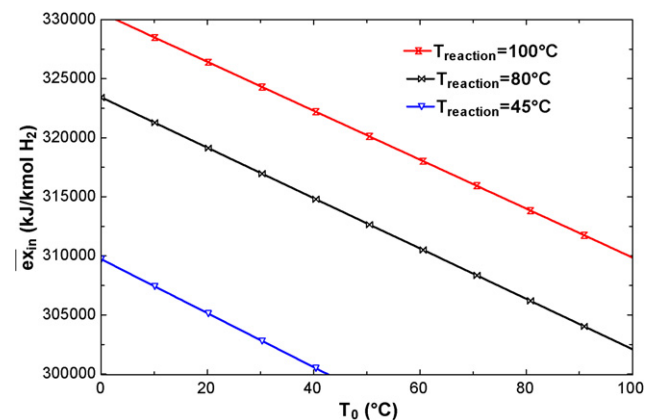

Fig. 8. Relation between reference-environment temperature and inlet exergy of the Cu production step at different reaction temperatures.
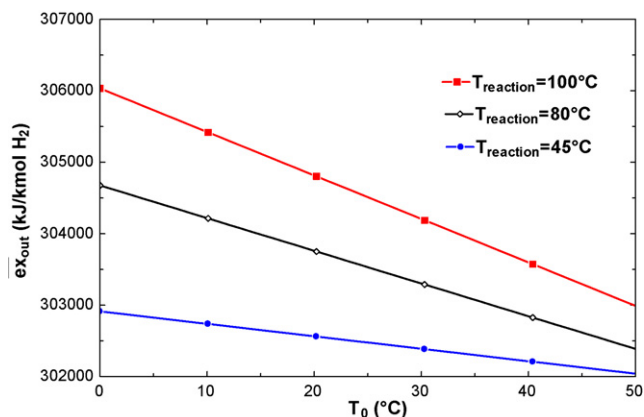
Fig. 9. Relation between reference-environment temperature and outlet exergy of the Cu production step at different reaction temperatures.
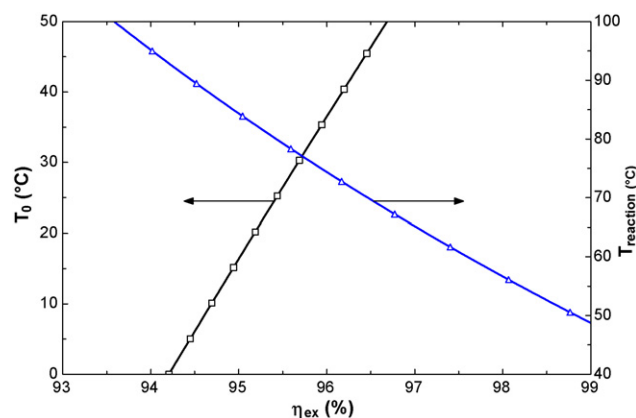

Fig. 10. Exergy efficiency of the Cu production step.

and the optimum values of these temperatures are not yet known. Thus, we provide a range, rather than a specific value, for the exergy efficiency. Although the efficiency of each step in the cycle is high, the overall efficiency of the cycle is low (below 50%), as expected.

Insufficient process data are available at present for a comprehensive detailed analysis, so this study focuses on identifying and characterizing general trends and sensitivities of the system using energy and exergy analyses, and can consequently be viewed as preliminary. In the future, as more actual data about the Cu–Cl cycle become available, through experimental investigations of the complete cycle (which are being carried out at UOIT) or via other means, the authors plan on carrying out a more detailed thermodynamic analysis, to extend the currently developed formulations and results. It is anticipated that these efforts will lead to a more comprehensive understanding of the cycle.

5. Conclusions

The energy and exergy analyses of the Cu production step of a Cu–Cl thermochemical cycle for hydrogen production performed in this article allow several conclusions to be drawn, which should assist efforts to understand the thermodynamic losses and efficiencies of the Cu production step and consequently to improve them and the overall cycle.

At a reaction temperature of $45\,°C$, the reaction heat of the Cu production step is $140{,}450\,kJ/kmol\ H_2$. The inlet

exergy of the step changes between $302{,}200\,kJ/kmol\ H_2$ and $305{,}000\,kJ/kmol\ H_2$, while the outlet exergy changes in the range of $302{,}100$–$302{,}600\,kJ/kmol\ H_2$ when the reference-environment temperature increases from $20\,°C$ to $40\,°C$ at a constant reaction temperature of $45\,°C$. Both inlet and outlet exergies decrease with reference-environment temperature. At a constant reaction temperature of $45\,°C$, the exergy destruction of the step varies between $50\,kJ/kmol\ H_2$ and $7000\,kJ/kmol\ H_2$ when the reference-environment temperature increases from $0\,°C$ to $30\,°C$. At a reaction temperature of $45\,°C$ and a reference-environment temperature of $25\,°C$, the exergy efficiency of this step is 99%. This efficiency decreases with increasing reference-environment temperature and with increasing reaction temperature.

The results of the energy and exergy analyses can be used to develop and assess measures to improve the process step, and in exergoeconomic and optimization analyses to reduce product costs and to increase the economic viability of the process. Various approximations, simplifications and assumptions have been used in this paper, in the absence of actual data for the Cu–Cl cycle. As a consequence, the energy or exergy results are not precise; rather the paper is intended to provide ranges of results and overall trends.

Acknowledgement

References

[1] M.A.K. Lodhi, Helio-hydro and helio-thermal production of hydrogen, International Journal of Hydrogen Energy 29 (2004) 1099–1113.
[2] N.N. Ponomarev-Stepnoi, Nuclear-hydrogen power, Atomic Energy 96 (2004) 375–385.
[3] K. Onuki, Y. Inagaki, R. Hino, Y. Tachibana, Research and development on nuclear hydrogen production using HTGR at JAERI, Progress in Nuclear Energy 47 (2005) 496–503.
[4] K. Verfondern, W.V. Lensa, Past and present research in Europe on the production of nuclear hydrogen with HTGR, Progress in Nuclear Energy 47 (2005) 472–483.
[5] F.M. Mitenkov, N.G. Kodochigov, A.V. Vasyaev, V.F. Golovko, N.N. Ponomarev-Stepnoi, N.E. Kukharkin, A.Y. Stolyarevskii, High-temperature gas-cooled reactors—energy source for industrial production of hydrogen, Atomic Energy 97 (2004) 829–840.
[6] C.W. Forsberg, Hydrogen, nuclear energy, and the advanced high-temperature reactor, International Journal of Hydrogen Energy 28 (2003) 1073–1081.
[7] T. Nishihara, Y. Inagaki, Development of control technology for the HTTR hydrogen production system, Nuclear Technology 153 (2006) 100–106.
[8] Y. Inagaki, H. Ohashi, Y. Inaba, H. Sato, T. Nishihara, T. Takeda, K. Hayashi, M. Ogawa, Research and development on system integration technology for connection of hydrogen production system to an HTGR, Nuclear Technology 157 (2007) 111–119.
[9] C.W. Forsberg, P.F. Peterson, P.S. Pickard, Molten salt-cooled advanced high temperature reactor for production of hydrogen and electricity, Nuclear Technology 144 (2003) 289–302.
[10] W. Xinxin, O. Kaoru, Thermochemical water splitting for hydrogen production utilizing nuclear heat from an HTGR, Tsinghua Science and Technology 10 (2005) 270–276.
[11] Y. Chikazawa, T. Nakagiri, M. Konomura, S. Uchida, Y. Tsuchiyama, A system design study of a fast breeder reactor hydrogen production plant using thermochemical and electrolytic hybrid process, Nuclear Technology 155 (2006) 340–349.
[12] M.A. Lewis, J.G. Masin, R.B. Vilim, Development of the low temperature Cu–Cl thermochemical cycle, in: International Congress on Advances in Nuclear Power Plants, Seoul, Korea, May 15–19, 2005.
[13] M.A. Lewis, M. Serban, J.K. Basco, Hydrogen production at <550 °C using a low temperature thermochemical cycle, in: Proceedings of the Nuclear Production of Hydrogen: Second Information Exchange Meeting, Argonne, IL, U.S., October 2–3, 2003, pp. 145–156.
[14] I. Dincer, M.A. Rosen, Exergy: Energy, Environment and Sustainable Development, Elsevier, London, 2007.
[15] National Institute of Standards and Technology (NIST), http://webbook.nist.gov/chemistry/, June 2005.